Electronic Supplementary Material (ESI) for Journal of Materials Chemistry A.

Supplementary information

Enhancement of pore confinement caused by mosaic structure on Ru nanoparticles for pH-universal hydrogen evolution reaction

Xiaofang Ma, He Xiao*, Yang Gao, Man Zhao, Li Zhang, Junming Zhang, Jianfeng Jia* and Haishun Wu

Key Laboratory of Magnetic Molecules & Magnetic Information Materials Ministry of Education, The School of Chemical and Material Science, Shanxi Normal University, Taiyuan 030000, China

*Corresponding author

E-mail:xiaohe200808@sxnu.edu.cn (H, Xiao); jiajf@dns.sxnu.edu.cn (J.F. Jia)

1 Some supplementary information during the experiment

The turnover frequency (TOF) values of the catalysts for the HER were calculated through the following equation:

TOF (s^{-1}) = (j×A)/(2×F×n).

In the formula, j ($A\cdot cm^{-2}$) is the current density at an overpotential of -100 mV, A = 0.07065 cm^{-2} is the geometric surface area of the glassy carbon electrode, F = 96,500 $C\cdot mol^{-1}$ is the Faraday constant, and n (mol) is the molar number of Ru loaded on the working electrode, which was calculated according to the result of ICP-OES.

The Faraday efficiency (FE) of the HER is determined using FE = n/(Q/2F), where F is the Faraday constant, n is the total amount of H_2, and Q is the total amount of charge obtained from the i-t curve.

2 Characterization techniques and other Supplements

Fig. S5 present the cyclic voltammetry (CV) curves of the Ru/HMCs-x recorded in the potential range of 0.346-0.446 V, 1.024-1.124 V and 0.611-0.711 V in 0.5 M H_2SO_4, 1 M KOH, and 0.5 M PBS with different scanning rates (e.g., 20, 40, 60, 80, 100, 120, 140, 160, 180 and 200 $mV\cdot s^{-1}$), respectively. According to the slope of the current density, which linearly changes with the increase in the scanning speed, the C_{dl} values of the corresponding catalyst can be calculated.[1] After extracting the C_{dl}

from the fitted linear regressions, we can calculate the electrochemically active surface area (ECSA) from the equation of ECSA = C_{dl}/C_s, where Cs are assumed to be same for all electrodes.[2]

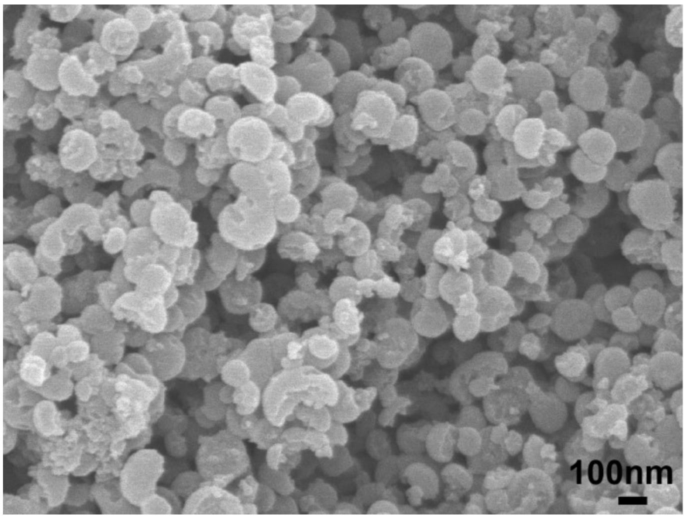

Fig. S1 SEM images of hollow mesoporous carbon spheres was prepared by adjusting PH= 11.5 with sodium hydroxide.

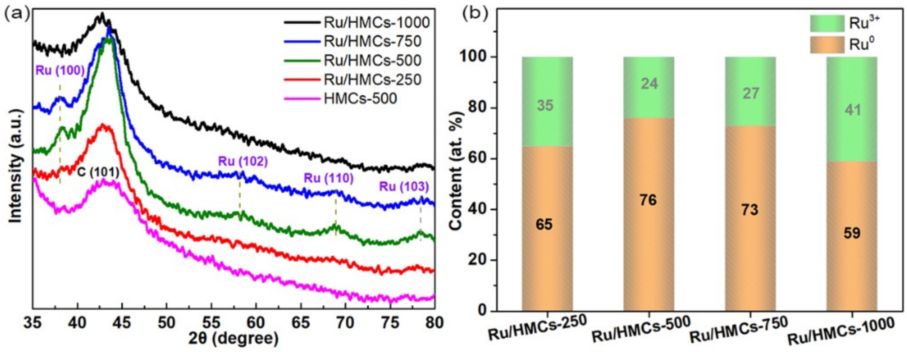

Fig. S2 (a) Local enlarged XRD images of Ru/HMCs-x and HMCs-500. (b) Relative contents comparison of Ru^0 and Ru^{3+} in as-prepared catalysts.

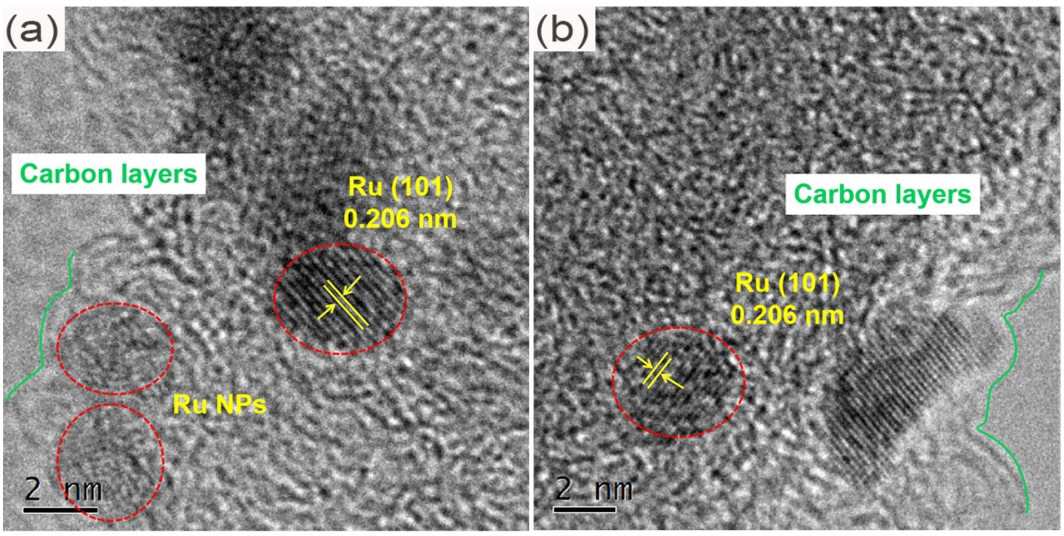

Fig. S3 HRTEM images of Ru/HMCs-500.

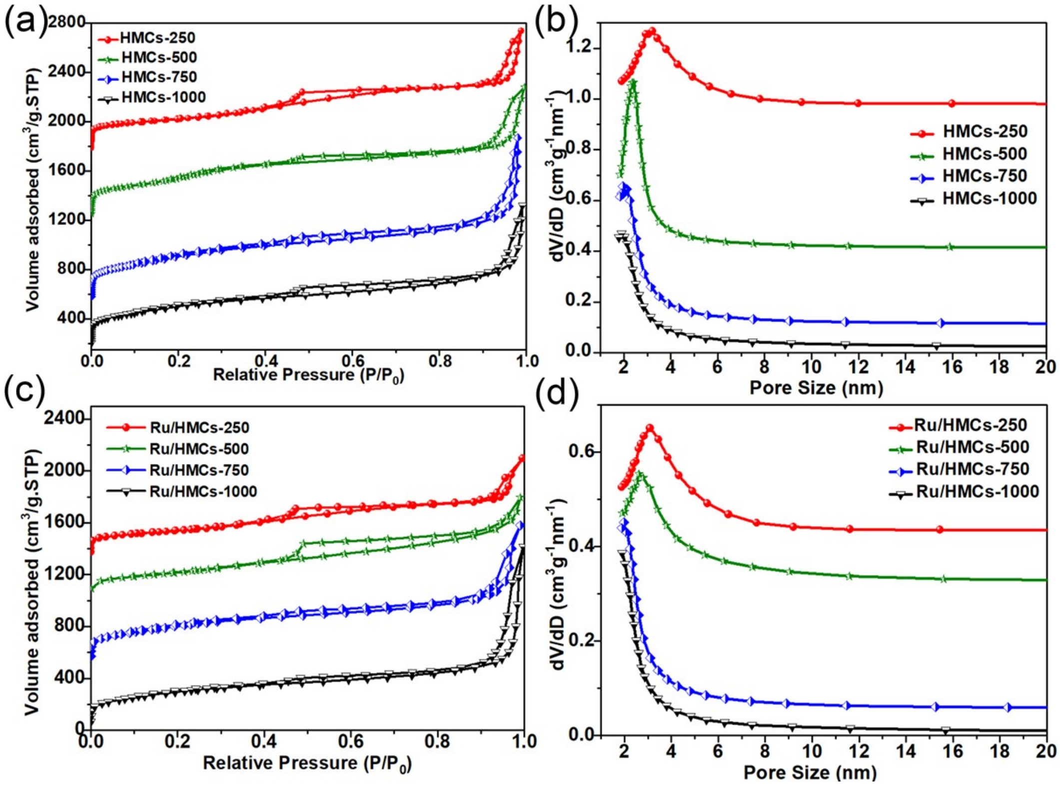

Fig. S4 N_2 adsorption and desorption isotherms of (a) HMCs-x and (c) Ru/HMCs-x. Pore size distribution of (b) HMCs-x and (d) Ru/HMCs-x.

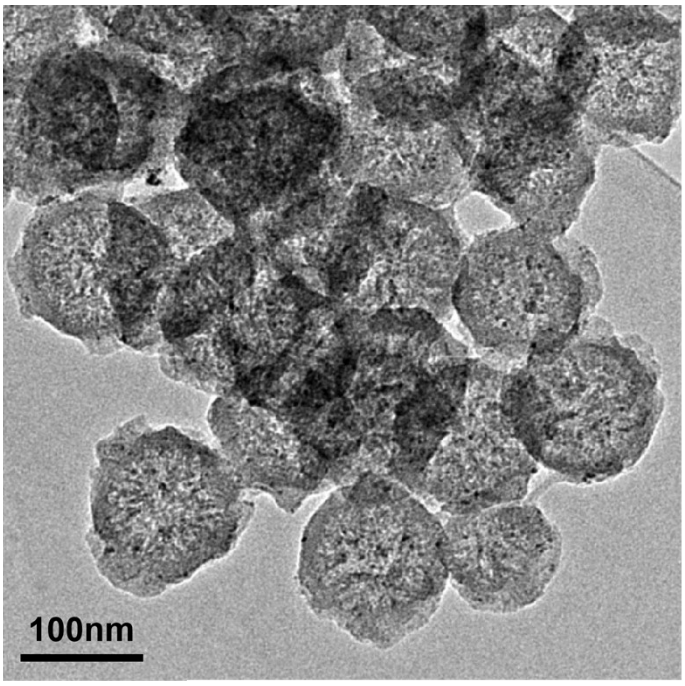

Fig. S5 TEM images of Ru/HMCs-500.

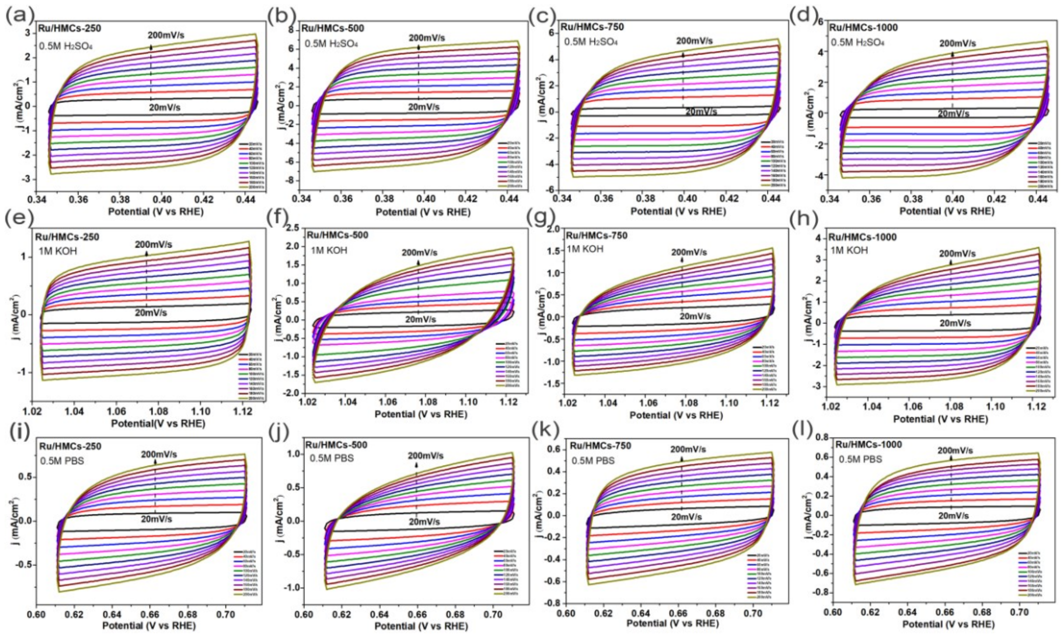

Fig. S6 Cyclic voltammetry curves of Ru/HMCs-x at scan rates from 20 to 200 mV s^{-1} in 0.5 M H_2SO_4, 1 M KOH, 0.5 M PBS, respectively. The differences in current density variation ($\Delta J = J_a - J_c$) at overpotential of 0.396 V, 1.074 V, and 0.661 V in acidic, alkaline, and neutral solutions plotted against the scan rate fitted to a linear regression enables the estimation of C_{dl}.

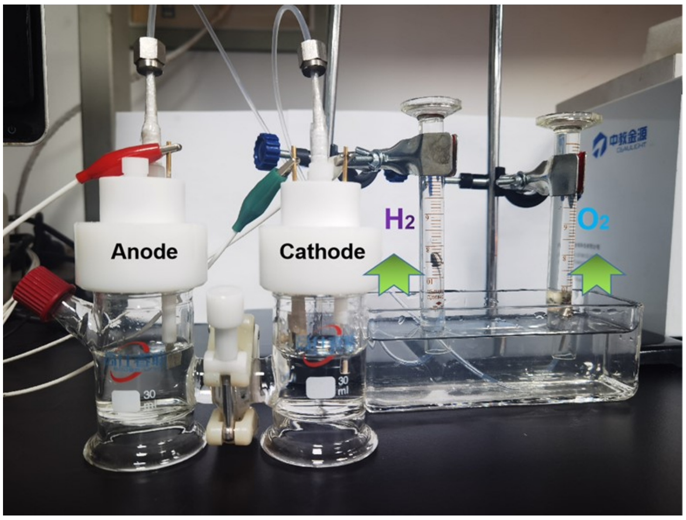

Fig. S7 Diagram of the device for collecting hydrogen and oxygen using the drainage gas collection method.

The two compartments of the airtight H-type electrolytic cell were separated by Nafion membrane, one of which was a catalyst-decorated carbon paper working electrode (geometric area 1 cm^2, catalyst loading 0.34 $mg \cdot cm^{-2}$) and Ag/AgCl reference electrode, the other chamber is the Pt sheet counter electrode. Under acidic and neutral conditions, the overpotential of 300 mV were tested for 10 min, and the released H_2 was collected by the drainage gas-gathering method (Fig. S6). Under alkaline conditions, due to the rapid hydrogen production, the overpotential was selected at 100 mV, and the amount of H_2 in the reaction for 10 min was collected.

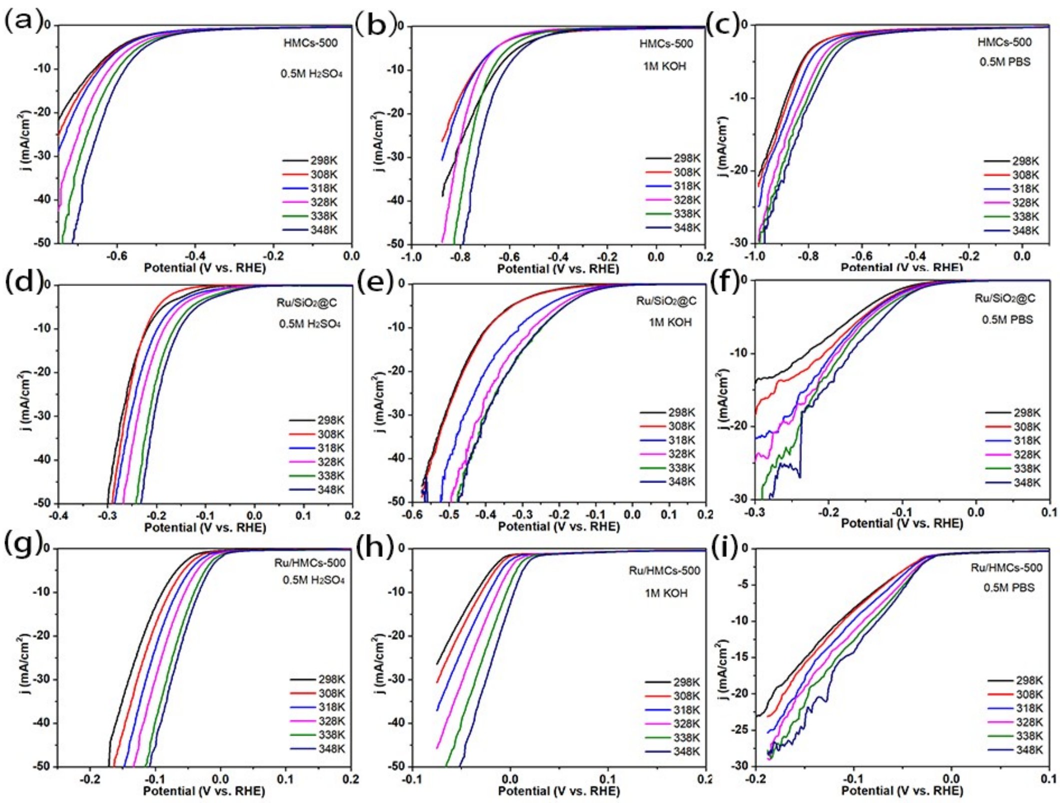

Fig.S8 Linear sweep voltammetry (LSV) curves of the catalysts in different electrolytes at temperatures from 25 to 75 °C for the hydrogen evolution reaction (HER). (a-c) HMCs-500, (d-f) Ru/SiO_2@C and (g-i) Ru/HMCs-500.

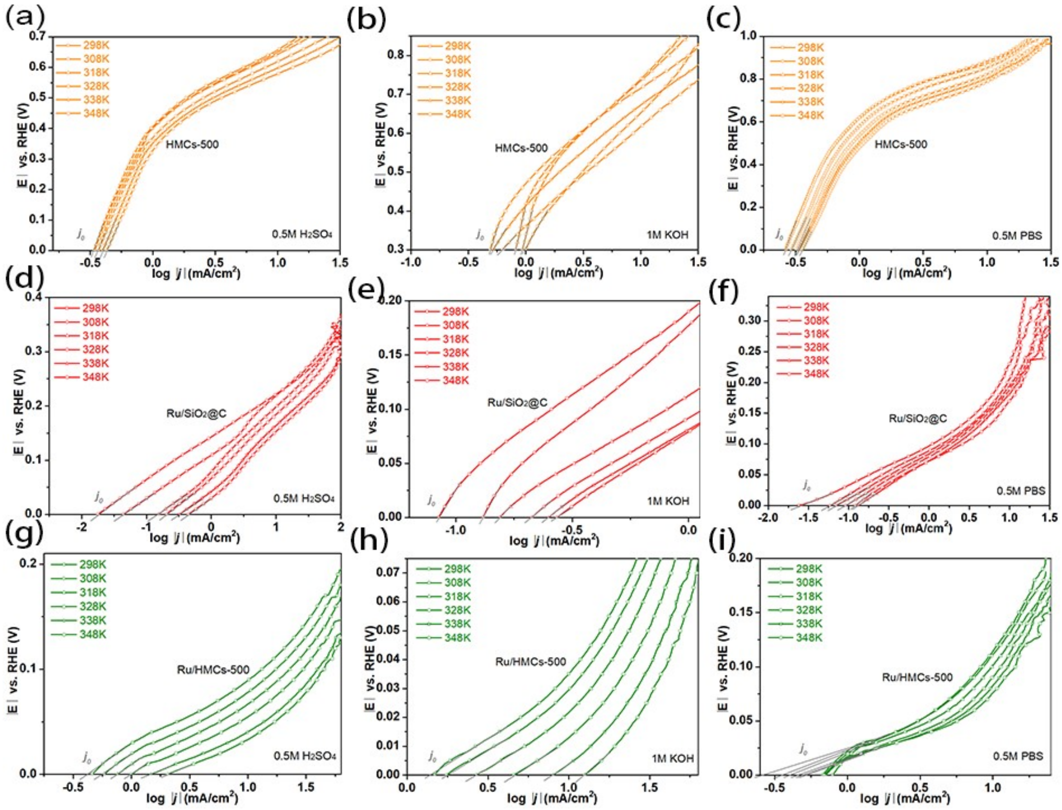

Fig. S9 Tafel curves of (a-c) HMCs-500, (d-f) $Ru/SiO_2@C$ and (g-i) Ru/HMCs-500 catalysts in different electrolytes at different temperatures ranging from 298 to 348 K. The exchange current density (j_0) was calculated by extending the linear part of Tafel plots.

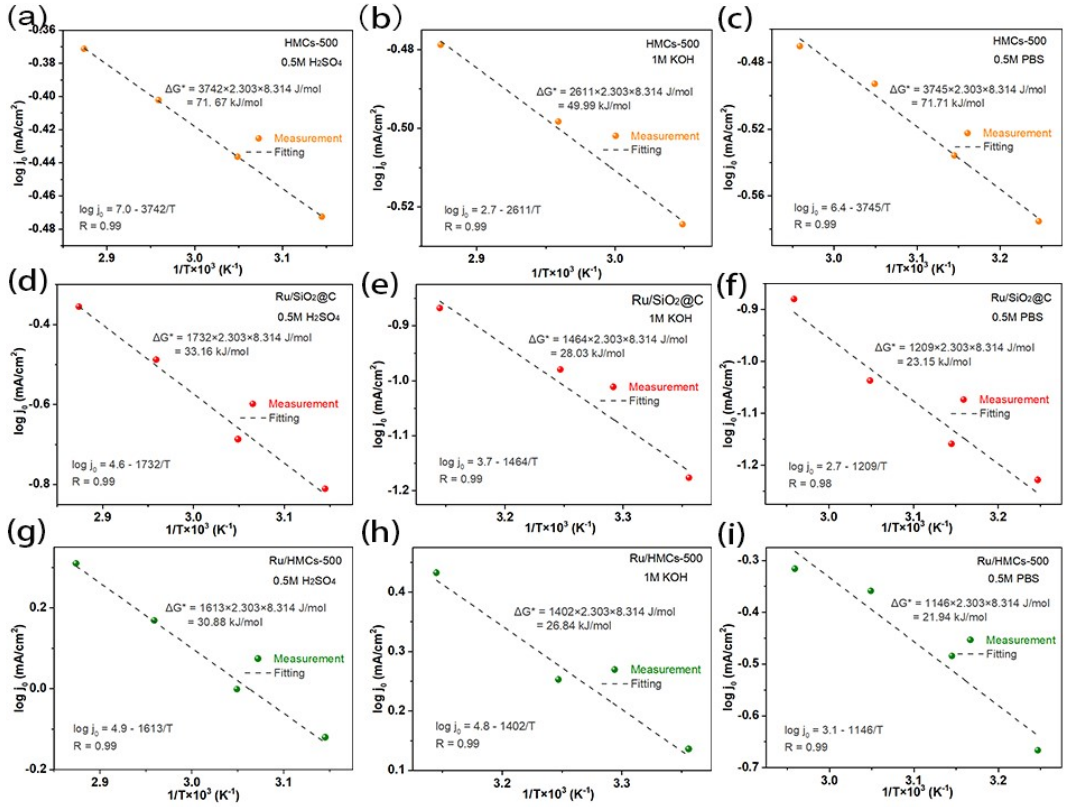

Fig. S10 Typical Arrhenius plots for the (a-c) HMCs-500, (d-f) $Ru/SiO_2@C$ and (g-i) Ru/HMCs-500 catalysts in different electrolyte solutions. The calculation of the ΔG* is based on the Arrhenius equation: $\log j_0 = \log (FKc) - \Delta G^*/2.303RT$.

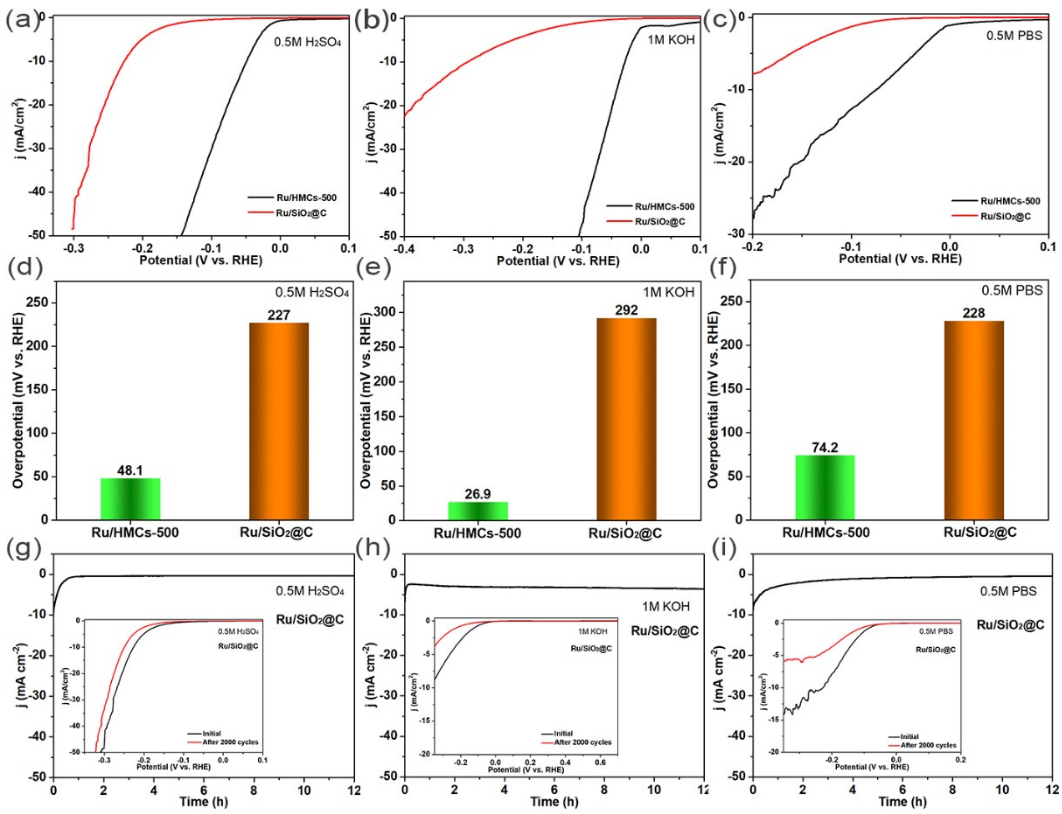

Fig. S11 (a-c) Comparison of HER performance of Ru/SiO_2@C and Ru/HMCs-500. (d-f) Histograms comparing overpotentials of Ru/HMCs-500 and Ru/SiO_2@C at 10 mA·cm^{-2} in different electrolytes. (g-i) The time-dependent current density curve of Ru/SiO_2@C. (inset: LSV curves of the Ru/SiO_2@C before and after 2000 CV cycles.)

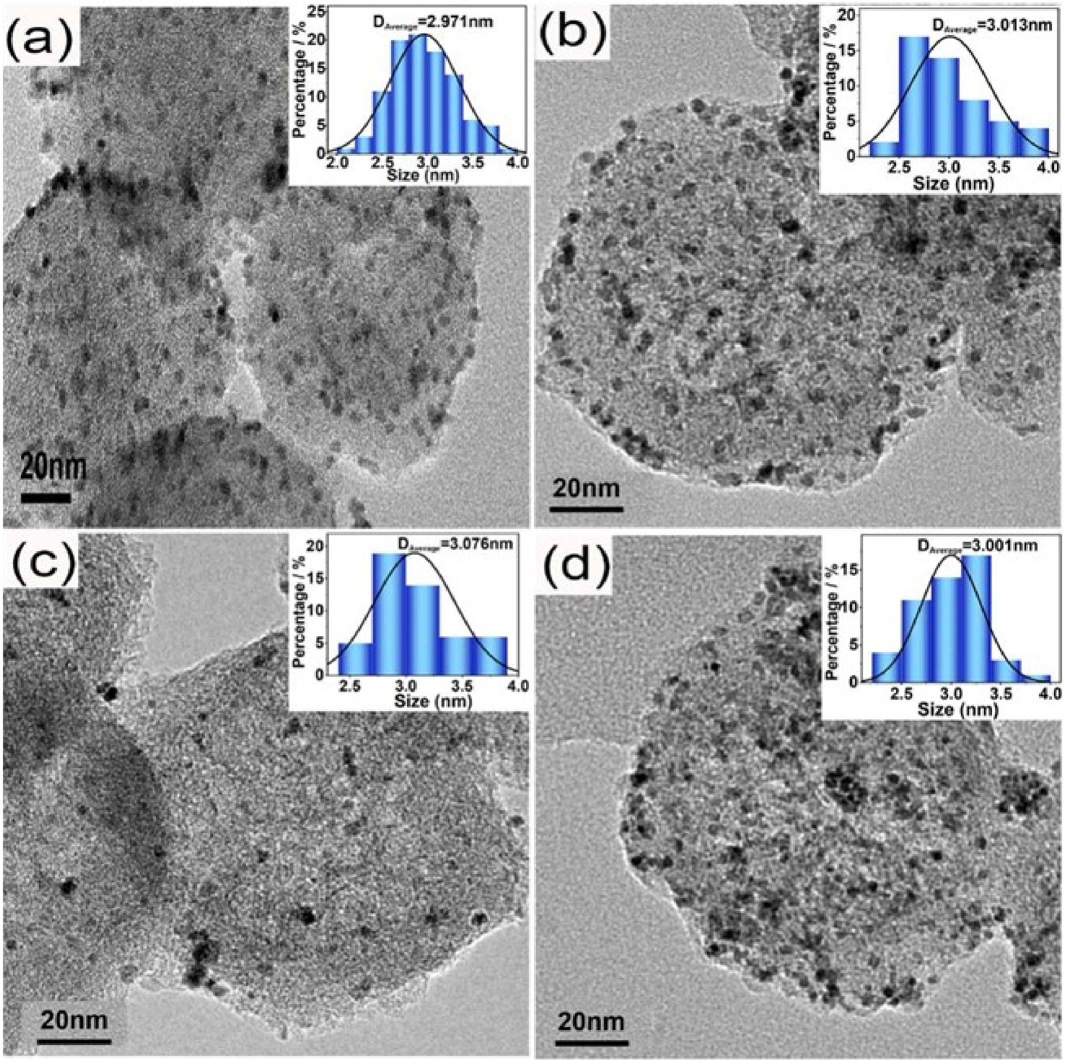

Fig. S12 TEM comparison of Ru/HMCs-500 before and after LSV test. (a) TEM image of Ru/HMCs-500 before testing. (b) TEM image after testing in 0.5 M H_2SO_4 solution, (c) in 1 M KOH solution and (d) in 0.5 M PBS solution. (Inset: Ru NPs size distribution images)

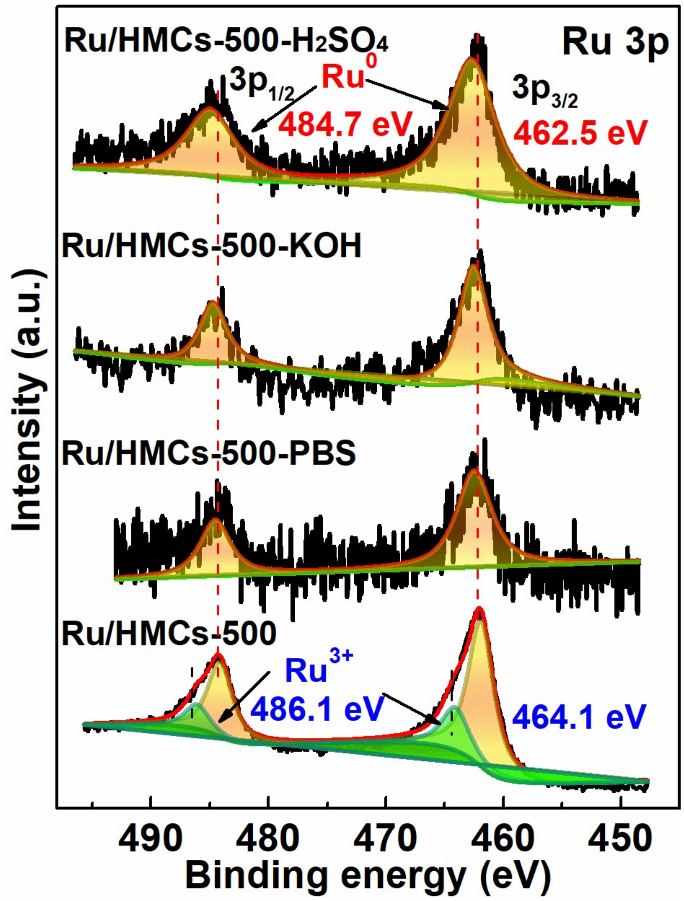

Fig. S13 Comparison of Ru 3p XPS peaks of Ru/HMCs-500 before and after LSV testing.

Table S1 EDS and ICP-OES data of Ru/HMCs-x samples.

Sample		Ru/HMCs-250	Ru/HMCs-500	Ru/HMCs-750	Ru/HMCs-1000
EDS	Ru wt.%	3.67	1.82	1.99	4.22
ICP-OES	Ru wt.%	4.26	3.75	4.34	4.65

Table S2 Textural Parameters of the Samples of HMCs-x and Ru/HMCs-x.

Sample	Average particle size (nm)	BET surface area (m^2 g^{-1})	Pore volume (cm^3 g^{-1})	Pore size (nm)
HMCs-250	121.3	861.4	1.51	3.21
HMCs-500	121.1	1177.1	1.71	2.42
HMCs-750	97.63	1260.6	2.04	1.96
HMCs-1000	98.31	1121.6	1.75	1.90
Ru/HMCs-250	131.2	680.9	1.19	3.09
Ru/HMCs-500	128.7	784.3	1.27	2.62
Ru/HMCs-750	110.2	984.7	1.61	1.97
Ru/HMCs-1000	100.3	947.5	2.08	1.90

Table S3 Comparison of HER performance in 1 M KOH for Ru/HMCs-500 with other HER electrocatalysts.

Reaction medium	Catalyst	η_{10}/mV	Tafel slope (mV dec^{-1})	Ref.
1 M KOH	Ru/HMCs-500	26.9	45.7	This work
	MoP-Ru_2P/NPC	47	36.9	[3]
	Ru-FeP	62	45	[4]
	Ru@Co/N-CNTs	48	45	[5]
	Co-Ru-MoS_2	52	55	[6]
	Ni_5P_4-Ru	54	52	[7]

Table S4 Comparison of HER performance in 0.5 M H_2SO_4 for Ru/HMCs-500 with other HER electrocatalysts.

Reaction medium	Catalyst	η_{10}/mV	Tafel slope (mV dec^{-1})	Ref.
0.5 M H_2SO_4	Ru/HMCs-500	48.09	38.99	This work
	Ru_xFe_y-NCs /CNF	66	43.44	[1]
	MoP-Ru_2P/NPC	82	64.99	[3]
	Ru@Co/N-CNTs	92	73	[5]
	ECM@Ru	63	47	[8]
	Ni@Ni_2P-Ru HNRs	51	35	[9]
	Ru@WNO-C	172	—	[10]
	$RuTe_2$/Gr	72	33	[11]

Table S5 Comparison of HER performance in 1 M PBS for Ru/HMCs-500 with other HER electrocatalysts.

Reaction medium	Catalyst	η_{10}/mV	Tafel slope (mV dec^{-1})	Ref.
1 M PBS	Ru/HMCs-500	71.1	53.0	This work
	MoP-Ru_2P/NPC	126	70.89	[3]
	RuP-475	47	45	[12]
	s-RuS_2/S-rGO	93	41	[13]
	RuP_2@NPC	57	87	[14]
	Ru/C-2	188	109	[15]
	RuP@NPC	110	59	[16]

References

1. B. Yang, J. Xu, D. Bin, J. Wang, J. Zhao, Y. Liu, B. Li, X. Fang, Y. Liu, L. Qiao, L. Liu and B. Liu, *Appl. Catal. B*, 2021, **238**, 119583.
2. J. Q. Chi, X. J. Zeng, X. Shang, B. Dong, Y. M. Chai, C. G. Liu, M. Marin and Y. Yin, *Adv. Funct. Mater.*, 2019, **29**, 1901790.
3. Y. Gao, Z. Chen, Y. Zhao, W. Yu, X. Jiang, M. He, Z. Li, T. Ma, Z. Wu and L. Wang, *Appl. Catal. B*, 2022, **303**, 120879.
4. H. Shang, Z. Zhao, J. Pei, Z. Jiang, D. Zhou, A. Li, J. Dong, P. An, L. Zheng and W. Chen, *J. Mater. Chem. A*, 2020, **8**, 22607-22612.
5. Z. Liu, X. Yang, G. Hu and L. Feng, *ACS Sustain. Chem. Eng.*, 2020, **8**, 9136-9144.
6. S. Kwon, T. T. Debela, I. H. Kwak, Y. C. Park, J. Seo, J. Y. Shim, S. J. Yoo, J. G. Kim, J. Park and H. S. Kang, *Small*, 2020, **16**, 2000081.
7. Q. He, D. Tian, H. Jiang, D. Cao, S. Wei, D. Liu, P. Song, Y. Lin and L. Song, *Adv. Mater.*, 2020, **32**, 1906972.
8. H. Zhang, W. Zhou, X. F. Lu, T. Chen and X. W. Lou, *Adv. Energy Mater.*, 2020, **10**, 2000882.
9. Y. Liu, Y. Liu, S. Liu, Y. Wang, Q. Zhang, L. Gu, S. Zhao, D. Xu, Y. Li, J. Bao and Z. Dai, J. *Am. Chem. Soc.*, 2018, **140**, 2731-2734.
10. G. Meng, H. Tian, L. Peng, Z. Ma, Y. Chen, C. Chen, Z. Chang, X. Cui and J. Shi, *Nano Energy*, 2021, **80**, 105531.
11. X. Gu, X. Yang and L. Feng, *Chem. Asian. J*, 2020, **15**, 2886-2891.
12. Q. Chang, J. Ma, Y. Zhu, Z. Li, D. Xu, X. Duan, W. Peng, Y. Li, G. Zhang, F. Zhang and X. Fan, *ACS Sustain. Chem. Eng.*, 2018, **6**, 6388-6394.
13. J. Yu, Y. Guo, S. Miao, M. Ni, W. Zhou and Z. Shao, *ACS Appl. Mater. Interfaces*, 2018, **10**, 34098-34107.
14. Z. Pu, I. S. Amiinu, Z. Kou, W. Li and S. Mu, *Angew. Chem. Int. Ed. Engl.*, 2017, **56,** 11559-11564.
15. H. Shi, L. Liu, Y. Shi, F. Liao, Y. Li and M. Shao, *Int. J. Hydrog. Energy*, 2019, **44**, 11817-11823.
16. J. Q. Chi, W. K. Gao, J. H. Lin, B. Dong, K. L. Yan, J. F. Qin, B. Liu, Y. M. Chai and C. G.

Liu, *ChemSusChem*, 2018, **11**, 743-752.